Indian Journal of Chemical Technology
Vol. 32, March 2025, pp. 246-253
DOI: 10.56042/ijct.v32i2.9819

Effect of system parameters on phase holdups for an inverse fluidized bed

Anup Kumar Swain[1]*, Abanti Sahoo[2], Hara Mohan Jena[2] & Hemalata Patra[3]

[1]Chemical Engineering Department, Indira Gandhi Institute of Technology, Sarang, Dhenkanal, Odisha – 759146, India

[2]Chemical Engineering Department, National Institute of Technology, Rourkela, Odisha – 769008, India

[3]CIPET: Institute of Petrochemicals Technology, B-25, CNI Complex, P.O. Patia, Bhubaneswar, Odisha - 751024, India

*E-mail: anup.k.swain@gmail.com

Received 22 March 2024; accepted 20 February 2025

Phase holdups for an inverse fluidized bed (IFB) have been studied using low density polypropylene (PP) particles for different system parameters viz. superficial gas velocities (U_g), ratio of bed volume to liquid (reactor) volume (V_b/V_r), and liquid recirculation velocities (U_{lr}). Gas phase holdup (ε_g) is found to increase with increase in U_g for all V_b/V_r ratios with and without liquid recirculation. Without liquid recirculation, ε_g decreased with increase in V_b/V_r ratio upto a certain V_b/V_r ratio for all U_g values and then increases with further increase in V_b/V_r ratios. While with liquid recirculation, ε_g is found to be higher than the case of without liquid recirculation. Liquid phase holdup (ε_l) and solid phase holdup (ε_s) are both found to decrease with increase in U_g for all V_b/V_r ratios with and without liquid recirculation. Regression analysis based mathematical correlations are developed to predict ε_g for different U_g, V_b/V_r, and U_{lr} values. Average absolute percent deviations of the developed correlations are found to be 7.90 and 7.39 which are less compared to the data available in the literature. Thus this study on phase holdups gives a clear insight providing a basis for the design of a three phase IFB reactor.

Keywords: Bed volume to liquid volume ratio, Gas phase holdup, Inverse fluidized bed, Liquid recirculation, Regression analysis, Superficial gas velocity

In conventional gas-liquid-solid fluidization systems, the density of solid particles is higher than the density of liquid phase. Here, fluidization of solid particles is in the vertically upward direction by the upward flow of gas and liquid phases. When the density of solid particles is less than the density of liquid phase, the solid particles float at the top of the liquid phase. In this case, fluidization of solid particles is in the vertically downward direction which is known as inverse fluidization. Here, inverse fluidization of solid particles can be achieved by two ways: upward flow of both gas and liquid phases or by a combination of upward flow of gas phase with downward flow of liquid phase[1,2].

Some of the major advantages of inverse fluidization systems include: higher gas phase holdups, greater heat and mass transfer rates, lesser bed pressure drops, superior stability, absence of clogging and channeling of the bed, lesser attrition of solid particles, ease of operation, easier to refluidize in case of electricity failure, lower consumption of electricity, and lower operating costs[1,2].

Hydrodynamic characteristics of inverse fluidization systems involving liquid-solid and gas-liquid-solid phases were first reported by Fan *et al*.[3]. Recent developments in hydrodynamic characteristics and different process aspects of inverse fluidization systems were well reviewed by Swain *et al*.[1], Arun *et al*.[4], and Sur and Mukhopadhyay[5]. Some of the important hydrodynamic characteristics of gas-liquid-solid inverse fluidization systems include: settled bed volume to reactor volume ratio, phase holdups, fluidization velocity, bed aspect ratio, superficial gas and liquid velocities, and bed expansion[5].

Gas, liquid, and solid phase holdups are important in determining the efficiency of the inverse fluidization systems. Phase holdups mainly depend on U_g, liquid viscosity (μ_l), particle density (ρ_s), and superficial liquid velocity (U_l)[6-9].

Fan *et al*.[3] observed the values of ε_g to be rising with the rising of U_g for lighter density polyethylene (PE) particles for both inverse bubbling and slugging fluidized bed regimes. It was also reported that in inverse bubbling fluidized bed regime, U_l have little effect on ε_g and in inverse slugging fluidized bed regime, with rise in U_l there is a rise in ε_g. Several other researchers also reported the rise of ε_g with rise in U_g[6,8-12]. Ibrahim *et al*. used PP particles in 5% (w) sodium chloride solution and observed a maximum ε_g near the bed height predicted from the profile of ε_s[13]. Hamdad *et al*. used PP particles in 0.5% (w) aqueous ethanol solution and in tap water and observed ε_g to be rising with rise in U_g but found ε_g to be higher in presence of ethanol than in tap water[14]. They also observed U_l to have negligible effect on ε_g. Sokół & Halfani observed ε_g to be rising with rise in U_g for PP particles for a given V_b/V_r ratio[12]. Sivasubramanian *et al*. used low density polyethylene (LDPE) particles in aqueous solutions of glycerol and carboxy methyl cellulose (CMC) and observed ε_g to be rising with rise in U_g, particle size, and concentrations of glycerol and CMC[15].

Values of ε_l were observed to rise slowly from the bed to the freeboard region over a wide range[13]. ε_l was observed to rise with the rise in U_g or U_l for both PE and PP particles. But at larger values of U_l, ε_l was found to be nearly constant[6]. Hamdad *et al*. found the maximum value of ε_l as 0.88 for a solid loading of 2.6 kg at U_g of 0.01 m/s which decreased slightly with the increase of U_g beyond 0.01 m/s. In presence of ethanol, values of ε_l were reduced[14]. Shin *et al*. used PE and PP particles to study the effect of liquid phase (solutions of CMC) viscosities on ε_l. For PE particles they observed that for lower values of U_l, the values of ε_l rises with rise in U_g and for higher values of U_l, ε_l exhibits a local maximum with the rise of U_g. For PP particles it was observed that ε_l rises with rise in U_l and U_g[9]. Sivasubramanian *et al*. observed ε_l to be increasing with increase in U_l[15].

Ibrahim *et al*. observed that the values of ε_s reduced from bed to freeboard regions[13]. Han *et al*. used hydrophobic and hydrophilic LDPE and medium density polyethylene (MDPE) particles in distilled water and they observed that the values of ε_s decreased with rise in U_g[16]. Shin *et al*. observed that values of ε_s decreased with rise in U_g, U_l, and μ_l[9]. For PP particles Bandaru *et al*. observed that values of ε_s reduced along the bed height with rise in U_l at constant U_g[17].

Some phase holdup correlations for inverse fluidization systems[3,9,18] are as follows:

$$\varepsilon_g = 5.517\, U_g^{0.383}\, U_l^{0.426}\, \mu_l^{-0.071}\left(\frac{\rho_s}{\rho_l}\right)^{11.357} \quad \text{... (1)}$$

$$\varepsilon_g = 0.71 U_g^{0.535} \quad \text{.... (2)}$$

$$\varepsilon_l = 4.014\, U_g^{0.136}\, U_l^{0.155}\, \mu_l^{0.056}\left(\frac{\rho_s}{\rho_l}\right)^{2.009} \quad \text{... (3)}$$

$$\varepsilon_s = \frac{M_s}{\rho_s\, A\, H} \quad \text{... (4)}$$

Where, ρ_l = liquid density (kg/m^3). M_s = mass of solid particles (kg), A = cross-sectional area of IFB column (m^2) and H = expanded bed height (m).

Ratio of settled bed height (H_s) to the column diameter (D) is called bed aspect ratio which rises with rise in H_s or decrease in D. For a particular column, changing the column diameter is difficult. Columns with lower aspect ratio require lower U_g for fluidization[18]. With the rise in H_s, higher U_g is required for achieving fluidization and with rise in V_b/V_r ratio, U_g was observed to increase[19].

Though these investigations provide useful information, they lack some aspects such as combined effect of several operating parameters i.e. U_g, U_l, V_b/V_r ratio, and small sized solid particles. Also there was no provision for recirculating the liquid phase. Modeling studies are also limited in these investigations. Keeping this in mind an IFB is used in the present study to find the effect of U_{lr} on phase holdups. Mathematical correlations for the prediction of ε_g have also been developed.

Experimental Section

Reactor setup and operation

An IFB (Fig. 1) with aspect ratio of 10:1 and total working volume of 10 L was used in this study. Through air-sparger and air-distributor plate, air was fed to the column from bottom while water was introduced from top. Compressed air and tap water were used in this study. To maintain the liquid level inside the column, a height-adjustable discharge pipe was attached to the column. Spherical PP particles of 920 kg/m^3 (density) and 5.63x10^{-3} m (average diameter) were used for the hydrodynamic study. For a particular bed volume (V_b), calculated mass of PP particles was taken inside the IFB. Liquid volume (V_r) is calculated from the height of liquid in IFB. U_g, U_{lr}, and V_b/V_r ratios were varied to estimate the ε_g. To achieve steady state between two successive set of readings, approximately 10 min time gap was maintained. To avoid build-up of excess pressure inside the IFB, an air vent was attached at the top. All the experiments were carried out in duplicate. The hydrodynamic parameters with their operating range are mentioned in Table 1.

Measurement of phase holdups

Volumetric method was used to measure ε_g due to its simplicity and no necessity of prior calibration[20].

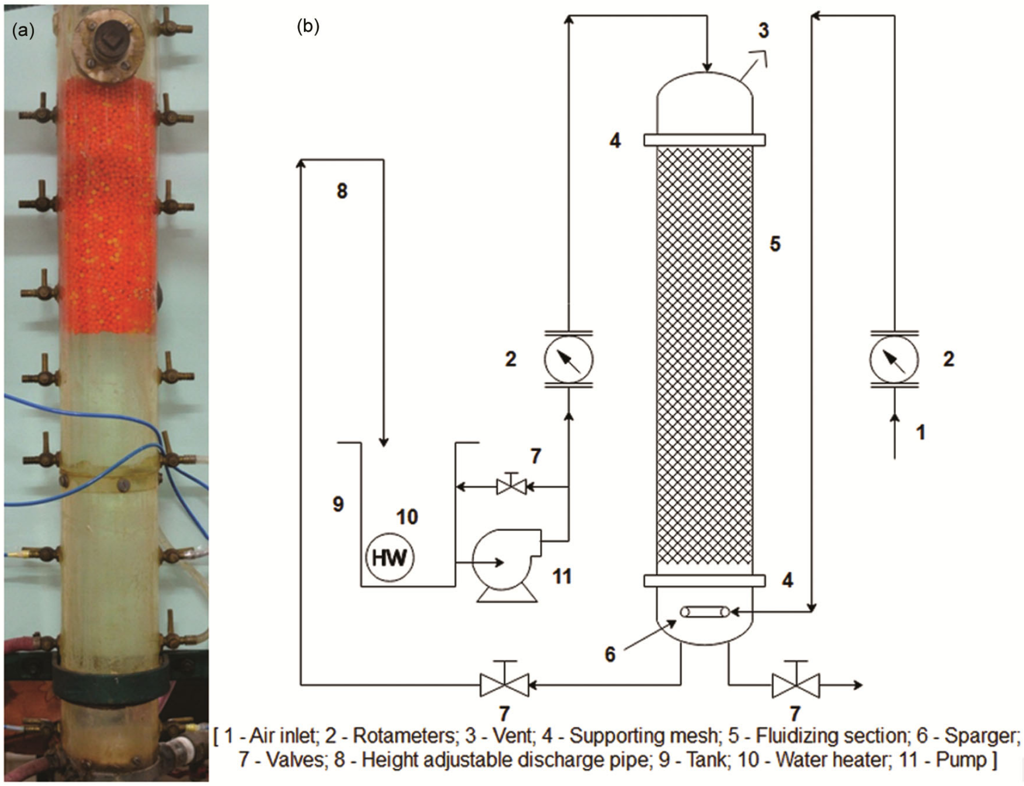

Fig. 1 — (a) Actual setup and (b) schematic representation of the IFB

Calculation of ε_g was based on the height difference between aerated and de-aerated liquid levels in the IFB. Eq. 5 was used to find out ε_g.

$$\varepsilon_g = \frac{H_a - H_d}{H_a} \quad \text{... (5)}$$

Where, H_a = height of aerated liquid (m) and H_d = height of de-aerated liquid (m).

Solid and liquid phase holdups were calculated using Eqs 4 and 6, respectively.

$$\varepsilon_l = 1 - (\varepsilon_g + \varepsilon_s) \quad \text{... (6)}$$

Model development for gas phase holdup

Using regression analysis technique, mathematical correlations were developed for the prediction of ε_g for different U_{lr} by taking different U_g and V_b/V_r ratios. Effect of system parameters (U_g and V_b/V_r ratio) for a certain U_{lr} on ε_g is studied by keeping one parameter constant while changing the other parameter and vice versa. Effect of one parameter (U_g or V_b/V_r ratios) on output ε_g is studied by plotting power law curves and the individual exponents of these power law curves are found. Then the overall effect of U_g and V_b/V_r ratios on output ε_g is studied by plotting power law curve and the overall exponent is found. Thereafter the correlation is developed as per the following format:

$$\varepsilon_g = K\,[A^{n1}B^{n2}]^n = K\,[A^{n1*n}B^{n2*n}] \quad \text{... (7)}$$

where, A and B are system parameters; n1 and n2 are individual exponents of A and B; and K and n are overall coefficient and overall exponent of the developed correlation, respectively.

Table 1 — Range of operating parameters for the hydrodynamic studies

Parameter	Range
V_b/V_r ratio	0.152 - 0.445
U_g	0.0043 - 0.0127 m/s
U_{lr}	0.0, 0.0021 m/s

Results and Discussion

Effect of U_g and V_b/V_r ratios on ε_g without liquid recirculation

Initially for no liquid recirculation, values of ε_g at different V_b/V_r ratios and U_g were measured (Fig. 2). It is seen that, ε_g rises with rise in U_g for all V_b/V_r ratios. This is due to the fact that with increase of U_g more air enters the IFB. Similar remarks were reported in published literatures[11,14]. ε_g is found to be higher for V_b/V_r ratios of 0.152 and 0.445 compared to other V_b/V_r ratios for all values of U_g. This happen

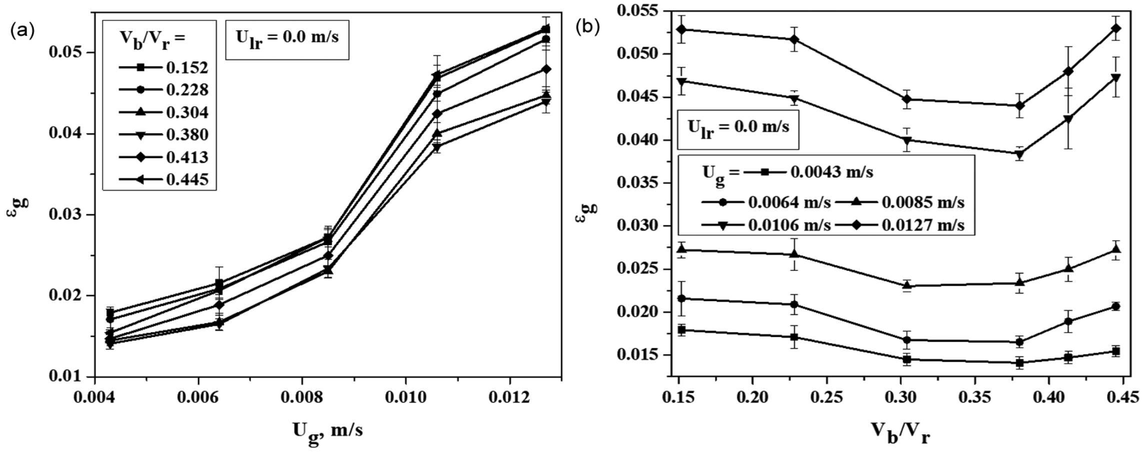

Fig. 2 — Effect of (a) U_g for different V_b/V_r ratios and (b) V_b/V_r ratios for different U_g on ε_g at U_{lr} = 0.0 m/s

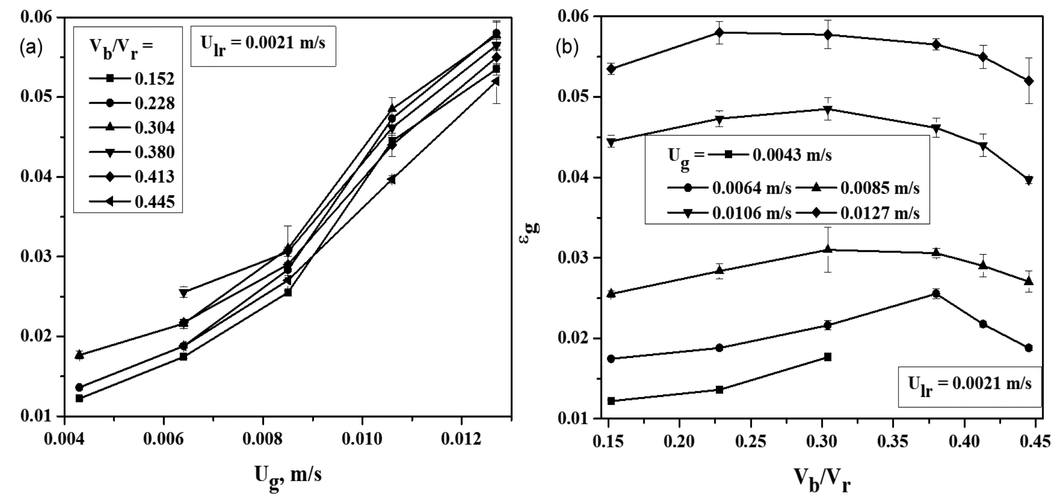

Fig. 3 — Effect of (a) U_g for different V_b/V_r ratios and (b) V_b/V_r ratios for different U_g on ε_g at U_{lr} = 0.0021 m/s

because at lower U_g values, the IFB with lower V_b/V_r ratios fluidizes faster than with higher V_b/V_r ratios. Here the bed voidage increases resulting into higher ε_g. While at higher U_g, all the solid particles for all V_b/V_r ratios fluidized downward as superficial velocity exceeds minimum fluidization velocity (U_{mf}). Values of ε_g decrease with the increase in V_b/V_r ratios from 0.152 to 0.380. It is minimum at V_b/V_r ratio of 0.380 for all values of U_g. For V_b/V_r ratios higher than 0.380, ε_g rises again because with increase in time the force on the lower part of bed is higher where solid particles are circulated vigorously. This fluidizes the whole bed thereby increasing the ε_g. This limiting point may be the condition of minimum fluidization.

Effect of U_g and V_b/V_r ratios on ε_g with liquid recirculation

Effect of U_g and V_b/V_r ratios with U_{lr} of 0.0021 m/s on ε_g is shown in Fig. 3. It is seen that with the increase in U_g, ε_g rises for all values of V_b/V_r ratios. The reason is as explained in previous section. Similar observations are found in literatures[10,21]. With the rise in V_b/V_r ratios for all values of U_g (except for 0.0043 m/s), ε_g rises then decreases with the rise in V_b/V_r ratios. At lowest U_g of 0.0043 m/s, fluidization of solid particles is not achieved for V_b/V_r ratios higher than 0.304. This is due to with liquid recirculation, lowest U_g of 0.0043 m/s is not enough to fluidize higher volumes (higher V_b/V_r ratios) of solid particles. At lower U_g of 0.0064 and 0.0085 m/s, maximum ε_g is seen at V_b/V_r ratios of 0.380 and 0.304 respectively. While at higher U_g of 0.0106 and 0.0127 m/s, maximum ε_g is seen at V_b/V_r ratios of 0.304 and 0.228, respectively. At these conditions, minimum fluidization condition might have been achieved. Beyond the minimum fluidization condition, ε_g reduces for all values of V_b/V_r ratios and U_g. For this reason, minimum ε_g is observed at V_b/V_r ratios of 0.152 and 0.445 at all values of U_g. Further it can be said that due to liquid recirculation, higher ε_g is observed with higher V_b/V_r ratios at lower U_g and with lower V_b/V_r ratios at higher U_g. This happens as more air is trapped at these conditions due to liquid recirculation. Also as U_g increases, minimum fluidization condition is observed at lower V_b/V_r ratios and vice versa.

U_{lr} above 0.0021 m/s created operational difficulties in controlling water level and air flow in IFB. For this reason, the hydrodynamic study is limited to U_{lr} of 0.0021 m/s only.

Effect of liquid recirculation velocities on ε_g

Upon comparison of ε_g values for different U_g and V_b/V_r ratios with and without liquid recirculation, ε_g is found to be higher with liquid recirculation condition for V_b/V_r ratios of 0.228 to 0.413 for all U_g values except for 0.0043 and 0.0064 m/s (Fig. 4). As particle density is less than water, they tend to move up in IFB. When liquid is recirculated from top, solid particles are forced to move downward while the upward flow of air, lift the solid particles upward. For this reason, hydrodynamic behaviour of solid particles with liquid recirculation is contrary to the case of without liquid recirculation. Some deviations are seen for V_b/V_r ratios of 0.152, 0.228, and 0.445 with lower U_g values of 0.0043 and 0.0064 m/s. This happens as less volume of air enters the IFB at lower U_g.

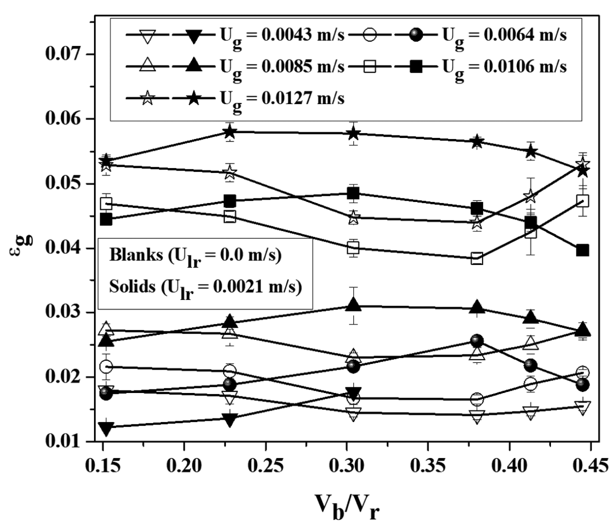

Fig. 4 — Effect of liquid recirculation on ε_g for different V_b/V_r ratios and U_g

Effect of U_g on ε_s with and without liquid recirculation

Effect of U_g on ε_s at U_{lr} of 0.0 and 0.0021 m/s is shown in Fig. 5. Without liquid recirculation conditions, it is seen that with the increase in U_g for all V_b/V_r ratios, ε_s drops. This is because with the rise in U_g, aerated height of bed (expanded bed height) of solid particles increases and from Eq. 4, ε_s is inversely related to aerated height. Similar remarks were found in literature[16]. Also with liquid recirculation similar effect is seen. Some deviations are observed for higher V_b/V_r ratios of 0.380 to 0.445 at U_g of 0.0043 m/s. This happens as the lowest U_g of 0.0043 m/s is unable to fluidize the solid particles having higher V_b/V_r ratios between 0.380 and 0.445.

Effect of U_g on ε_l with and without liquid recirculation

Effect of U_g on ε_l at U_{lr} of 0.0 and 0.0021 m/s is shown in Fig. 6. At both conditions, ε_l decreases with rise in U_g for all V_b/V_r ratios. This happens as with the increase in U_g, the ε_g rises and from Eq. 6 it is obvious that as ε_g rises, the ε_l value decreases. Similar views are also found in literatures[15,16].

Models for gas phase holdup

Based on regression analysis technique, the developed model equations for ε_g for U_{lr} of 0.0 and 0.0021 m/s are mentioned in Eqs 8 and 9, respectively. Their correlation plots are shown in Fig. 7. In Table 2,

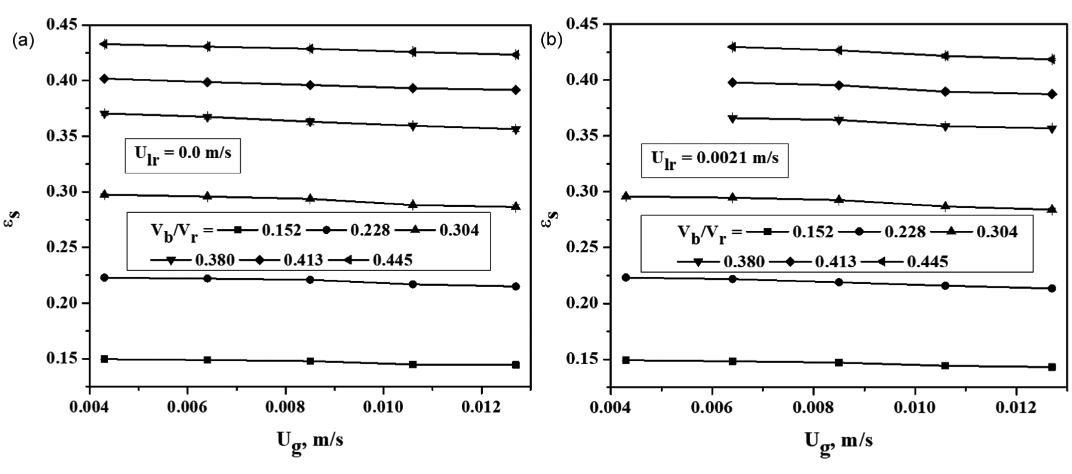

Fig. 5 — Effect of U_g on ε_s: (a) without and (b) with liquid recirculation

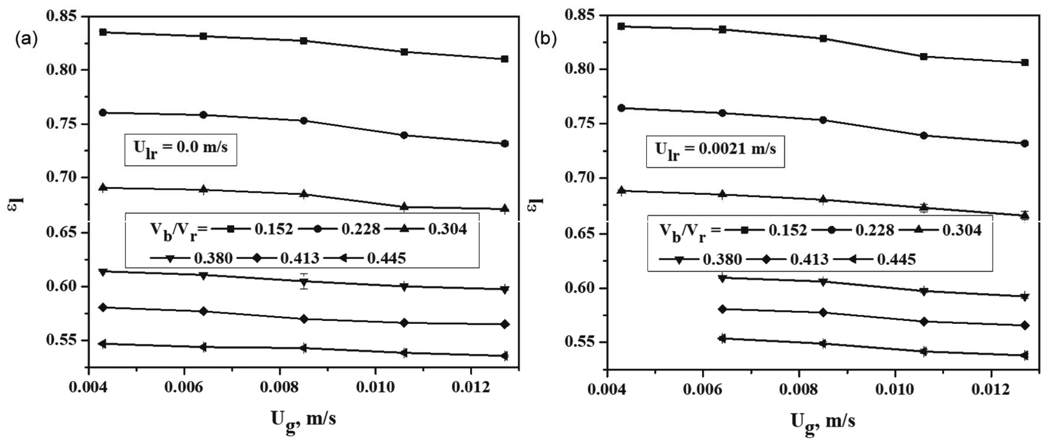

Fig. 6 — Effect of U_g on ε_l; (a) without and (b) with liquid recirculation

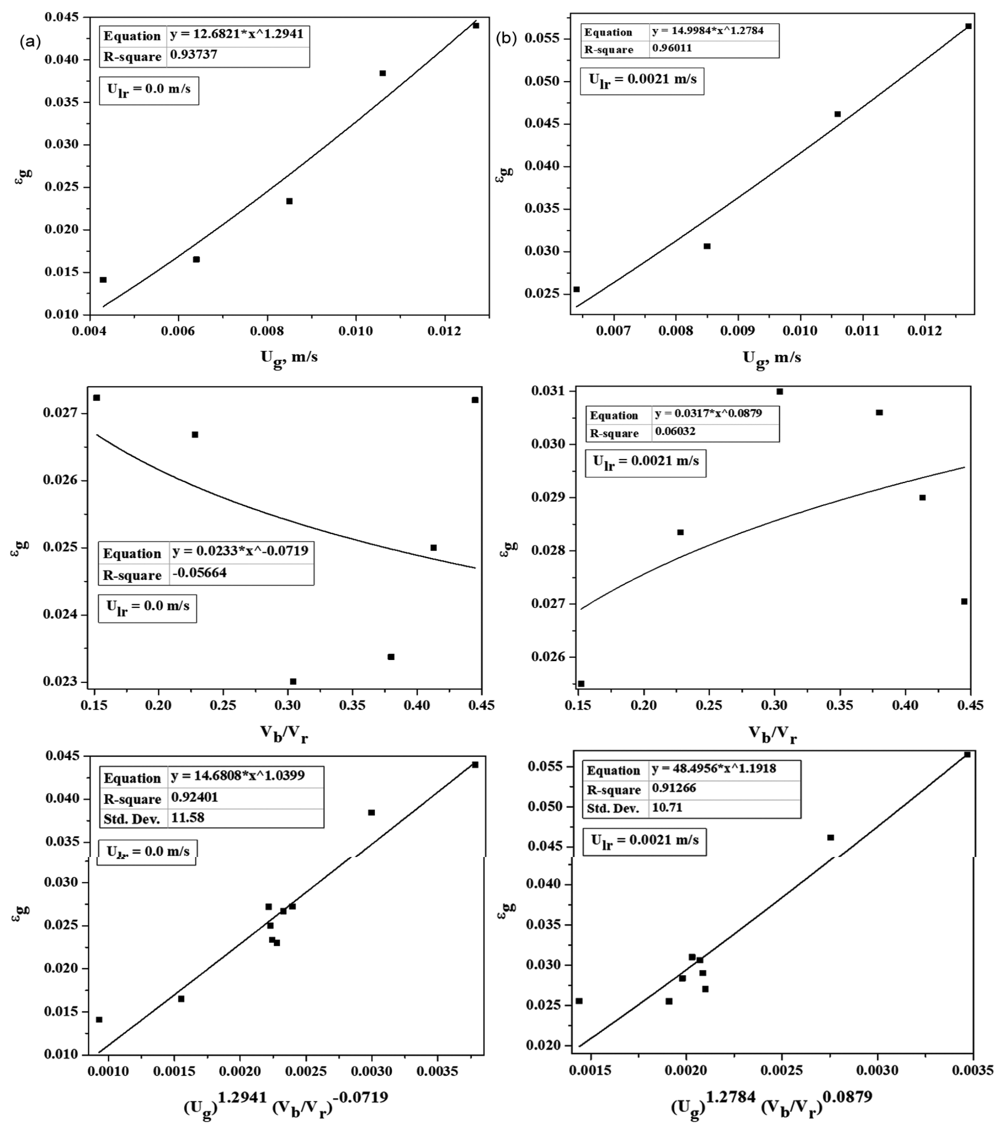

Fig. 7 — Correlation plots of ε_g at different liquid recirculation conditions

Table 2 — Average absolute percent deviation of the predicted values for ε_g from the experimental values by various correlations

Corrections	Reference	Average absolute percent deviation
$\varepsilon_g = 5.517\ U_g^{0.383}\ U_l^{0.426}\ \mu_l^{-0.071}\left(\frac{\rho_s}{\rho_l}\right)^{11.357}$	9	30.21
$\varepsilon_g = 0.71\ U_g^{0.535}$	18	55.99
$\varepsilon_g = 14.6808\ U_g^{1.3457}\left(\frac{V_b}{V_r}\right)^{-0.0747}$ (for U_{lr} = 0.0 m/s)	Present study	7.90
$\varepsilon_g = 48.4956\ U_g^{1.5236}\left(\frac{V_b}{V_r}\right)^{0.1047}$ (for U_{lr} = 0.0021 m/s)	Present study	7.39

average absolute percentage deviations of the predicted values for ε_g from the experimental values by various correlations are presented.

$$\varepsilon_g = 14.6808\,(U_g)^{1.3457}\left(\frac{V_b}{V_r}\right)^{-0.0747} (\text{for } U_{lr} = 0.0 \text{ m/s}) \quad \ldots (8)$$

$$\varepsilon_g = 48.4956\,(U_g)^{1.5236}\left(\frac{V_b}{V_r}\right)^{0.1047} (\text{for } U_{lr} = 0.0021 \text{ m/s}) \quad \ldots (9)$$

Based on R^2 and standard deviation values obtained from Fig. 7, the developed correlations can be said to be significant. It is observed from Table 2, that the developed correlations have less average absolute percent deviations compared to relatively high average absolute percent deviations for other correlations. This may be due to different dimensions of IFB and range of parameters taken. Developed correlations have a new parameter called V_b/V_r ratio which was not used in previously published correlations. Developed correlations can be used over a wide range of U_g and V_b/V_r ratios.

Conclusion

From the hydrodynamic study in the present IFB, it is found that ε_g increases with the increase in U_g for all V_b/V_r ratios for both U_{lr} values of 0.0 and 0.0021 m/s. ε_g values were found to be higher with liquid recirculation than without liquid recirculation and the maximum increase in ε_g is observed for V_b/V_r ratios of 0.304 and 0.380 at U_g between 0.0085 to 0.0127 m/s. With liquid recirculation in IFB, when U_g is increased from 0.0085 to 0.0127 m/s for V_b/V_r ratio of 0.304, ε_g values increased between 34.72 and 29.05% respectively over without liquid recirculation condition. While the increase in ε_g for V_b/V_r ratio of 0.380 is between 30.93 and 28.42%. Thus, it is better to operate the present IFB with V_b/V_r ratios between 0.228 to 0.413 at U_g above 0.0085 m/s and U_{lr} of 0.0021 m/s for getting maximum ε_g. These results are very encouraging from bioreactor point of view because higher ε_g is desired for growth of microorganisms. Both liquid and solid phase holdups were found to decrease with increase in U_g. The developed correlations for ε_g having with average absolute percent deviations of 7.39 to 7.90 suggest their suitability for the prediction of ε_g over a wide range of parameters. The observations from this study will be highly useful for the design of a three phase IFB reactor.

References

1 Swain A K, Sahoo A, Jena H M & Patra H, Industrial wastewater treatment by aerobic inverse fluidized bed biofilm reactors (AIFBBRs): A review, *J Water Process Eng*, 23 (2018) 61.

2 Swain A K, Sahoo A, Jena H M & Bhuyan S C, Effect of superficial gas velocity and ratio of bed volume to reactor volume of inverse fluidized bed biofilm reactor on the removal of ammonia-nitrogen from wastewater, *Indian J Chem Technol*, 28 (2021) 709.

3 Fan L S, Muroyama K & Chern S H, Hydrodynamic characteristics of inverse fluidization in liquid-solid and gas-liquid-solid systems, *Chem Eng J*, 24 (1982) 143.

4 Arun A N, Razack A A & Sivasubramanian V, Recent progress in hydrodynamics of inverse fluidized bed reactors: A review, *Chem Eng Commun*, 200 (2013) 1260.

5 Sur D H & Mukhopadhyay M, Process aspects of three-phase inverse fluidized bed bioreactor: A review, *J Environ Chem Eng*, 5 (2017) 3518.

6 Cho Y J, Park H Y, Kim S W & Kang Y, Heat transfer and hydrodynamics in two- and three-phase inverse fluidized beds, *Ind Eng Chem Res*, 41 (2002) 2058.

7 Kim S D & Kang Y, Hydrodynamics, heat and mass transfer in inverse and circulating three-phase fluidized-bed reactors for wastewater treatment, *Stud Surf Sci Catal*, 159 (2006) 103.

8 Liu M, Lu C, Shi M, Ge B & Huang J, Hydrodynamics and mass transfer in a modified three-phase airlift loop reactor, *Pet Sci*, 4 (2007) 91.

9 Shin I S, Son S M, Kang Y, Kang S H & Kim S D, Phase holdup characteristics of viscous three-phase inverse fluidized beds, *J Ind Eng Chem*, 13 (2007) 971.

10 Lee D H, Epstein N & Grace J R, Hydrodynamic transition from fixed to fully fluidized beds for three-phase inverse fluidization, *Korean J Chem Eng*, 17 (2000) 684.

11 Myre D & Macchi A, Heat transfer and bubble dynamics in a three-phase inverse fluidized bed, *Chem Eng Process - Process Intensif*, 49 (2010) 523.

12 Sokół W & Halfani M R, Hydrodynamics of a gas-liquid-solid fluidised bed bioreactor with a low density biomass support, *Biochem Eng J*, 3 (1999) 185.

13 Ibrahim Y A A, Briens C L, Margaritis A & Bergongnou M A, Hydrodynamic characteristics of a three-phase inverse fluidized-bed column, *AIChE J*, 42 (1996) 1889.

14 Hamdad I, Hashemi S, Rossi D & Macchi A, Oxygen transfer and hydrodynamics in three-phase inverse fluidized beds, *Chem Eng Sci*, 62 (2007) 7399.

15 Sivasubramanian V, Velan M & Haribabu K, Holdup studies in IFBR for wastewater treatment, *J Adv Eng Res*, 1 (2014) 8.

16 Han H D, Lee W, Kim Y K, Kwon J L, Choi H S, Kang Y & Kim S D, Phase hold-up and critical fluidization velocity in a three-phase inverse fluidized bed, *Korean J Chem Eng*, 20 (2003) 163.

17 Bandaru K S V S R, Murthy D V S & Krishnaiah K, Some hydrodynamic aspects of 3-phase inverse fluidized bed, *China Particuol*, 5 (2007) 351.

18 Ochieng A, Odiyo J O & Mutsago M, Biological treatment of mixed industrial wastewaters in a fluidised bed reactor, *J Hazard Mater*, B96 (2003) 79.

19 Swain A K, *Studies on Removal of Ammonia-Nitrogen from Industrial Wastewater using Inverse Fluidized Bed Biofilm Reactor*, Ph.D. Thesis, National Institute of Technology, Rourkela, (2021).

20 Euzen J P, Trambouze P & Wauquier J P, *Scale-up Methodology for Chemical Processes* (Editions Technip, Paris), (1993).

21 Buffière P & Moletta R, Some hydrodynamic characteristics of inverse three phase fluidized-bed reactors, *Chem Eng Sci*, 54 (1999) 1233.